Structural Chemistry (2023) 34:713–722
https://doi.org/10.1007/s11224-022-02017-8

ORIGINAL RESEARCH

NMR and computational studies of ammonium ion binding to dibenzo-18-crown-6

Brielle Shope[1,5] · D. Brandon Magers[1,2] · István Pelczer[3] · David Řeha[4] · Babak Minofar[4] · Jannette Carey[3,4]

Received: 22 March 2022 / Accepted: 8 July 2022 / Published online: 20 July 2022

Abstract

Dibenzo-18-crown-6 (DB18C6) is a single-crown ether that can act as a host for a guest ion. In an effort to illuminate the relationships among structure, dynamics, and thermodynamics of ligand binding in a simple model for understanding the affinity and specificity of ligand interactions, nuclear magnetic resonance (NMR) experiments and density functional theory (DFT) were used to study the interaction of DB18C6 with ammonium ion. ^{1}H-NMR was used to follow the titration of DB18C6 with ammonium chloride in deuterated methanol, a solvent chosen for its amphipathic character. Ammonium ion binds strongly to DB18C6 with a dissociation equilibrium constant at least as low as ~ 10^{-6} M. DFT calculations were used to identify optimized conformations of bound and free DB18C6 and to estimate its binding energy with ammonium ion in implicit solvent. An approach is described that accounts for geometry relaxation in addition to solvation correction and basis set superposition error; to our knowledge, this is the first such report that includes the energy difference from optimizing species geometry. The lowest-energy conformer of free DB18C6 in implicit methanol acquires an open, W-shaped structure that is also the lowest-energy conformer found for the DB18C6-ammonium ion complex. These results form a foundation for further studies of this system by molecular dynamics simulations.

Keywords Host–guest systems · Ligand-binding affinity · Forward and reverse titration · Molar ratio of binding · Stoichiometric titration · Conformational transitions · Synergy of experiment and computation

Introduction

In 1987, Lehn, Cram, and Pedersen won the Nobel Prize in chemistry for the understanding of ligand-binding affinity and specificity they developed through their work on crown ethers. Crown ethers are cyclic compounds that can act as hosts with high affinity and protein-like selectivity for guest compounds. The first crown ether studied, dibenzo-18-crown-6 (DB18C6), showed binding of cations that was quite strong for a neutral molecule [1, 2]. This crown ether has a benzene ring on each side of a central cyclic polyether ring containing eight carbons and six oxygen atoms. The structure and complexation of DB18C6 with ammonium ion are shown in Fig. 1. The two-dimensional view suggests that partial negative charges of multiple oxygen atoms all pointing in toward the central cavity attract positively charged ions. Pedersen and Frensdorff studied DB18C6 and its complexation with ions including NH_4^+, K^+, and Na^+, finding that K^+ binds to DB18C6 with a dissociation equilibrium constant, K_d, of 4×10^{-6} M in dichloromethane at room temperature [3]. They reported that ammonium ion also binds well with cyclic polyethers including DB18C6 [3] but did not report its affinity for DB18C6. Since then, extensive

Brielle Shope and D. Brandon Magers contributed equally to this work.

✉ D. Brandon Magers
bmagers@belhaven.edu

✉ Jannette Carey
jcarey@princeton.edu

1 Department of Chemistry, Taylor University, Upland, IN 46989, USA

2 Department of Chemistry and Physics, Belhaven University, Jackson, MS 39202, USA

3 Department of Chemistry, Princeton University, Princeton, NJ 08544, USA

4 Laboratory of Structural Biology and Bioinformatics, Institute of Microbiology of the Czech Academy of Sciences, Zamek 136, 37333 Nové Hrady, Czech Republic

5 Department of Chemistry, University of Virginia, Charlottesville, VA 22904, USA

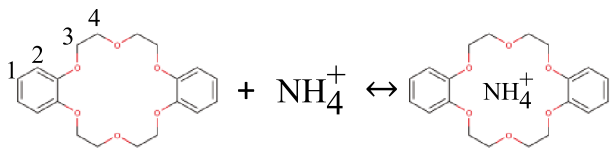

Fig. 1 Structure of DB18C6 and binding with ammonium ion. Oxygen atoms are colored red. Numbers adjacent to each unique carbon atom indicate NMR assignments (see Fig. 2)

thermodynamic data have been accumulated for binding of ions to DB18C6 and other cyclic polyethers in various solvents [4–8]. Shchori et al. reported stability constants for nitrate and chloride salts including NH_4Cl binding to DB18C6 in CCl_4 [6]. Angelis et al. used electrochemistry to calculate reaction rates and stability constants of NH_4^+ binding to DB18C6 in acetonitrile [7]. Izutsu et al. calculated formation constants for DB18C6 with NH_4^+ in acetonitrile [8].

The above studies together report stability constants, reaction rates, and/or formation constants for ammonium ion binding to DB18C6 in acetonitrile or CCl_4. To the best of the authors' knowledge, no quantitative experimental analysis of binding affinity has been reported for complexation of simple salts like ammonium chloride with DB18C6 in more polar solvents, where binding thermodynamics are expected to be dominated by solvent contributions and thus may more closely mimic protein–ligand interactions. However, other cyclic polyethers are reported to form weak complexes in aqueous solution, with stability constants three to four orders of magnitude weaker than in methanol [9]. This result is consistent with the expectation that water competes more effectively than methanol for the free cation, but it makes experimental studies in water inaccessible due to low affinity. To begin to fill this knowledge gap, the present study was carried out in methanol to augment our understanding of the thermodynamic forces at work in binding of a model cation to DB18C6 under conditions where experimentally observable binding occurs. Complexation was monitored using proton nuclear magnetic resonance spectroscopy (^{1}H-NMR) [10, 11]. Selection of the nitrogen-containing ammonium ion also offered the potential for complementary detection of binding by using ^{15}N NMR with isotope-labeled ligand, although the results from ^{1}H-NMR reported here fully resolve the quantitative parameters of the binding process without requiring the use of ^{15}N NMR.

Due to their single bonds, crown ethers can take on many conformations in solution. Computational studies have explored the conformations of DB18C6 when empty or complexed with various cations [12–16]. Bright and Truter carried out x-ray crystal structure analysis of DB18C6 complexed with 55:45 rubidium:sodium isothiocyanate, finding that the complexed and uncomplexed crystal structure conformations of DB18C6 differ. The complexed ether oxygen were found to be almost coplanar (deviation 0.08 Å), and the uncomplexed ether oxygens have 100% larger deviation (deviation 0.16 Å). The center of the uncomplexed ether is at a crystallographic center of symmetry, but the three oxygen atoms on one side of the complexed crown are not equidistant from the symmetry center, so the cation makes unequal contact with the six oxygen atoms [14, 17]. Kríž et al. studied the interaction of H_3O^+ with DB18C6 in nitrobenzene-d_5 and dichloromethane-d_2 through NMR, FTIR, and density functional theory (DFT) calculations to establish the most stable electronic structures [15]. The most energetically favored conformer in the gas phase for both the complexed and uncomplexed crowns has apparent C_{2v} symmetry with a structure seemingly identical to the W-shaped lowest-energy structure reported in the present work. However, the prior DFT calculations were made entirely in the gas phase, and Kríž et al. reported no results in solvent.

In the work reported here, the conformations of uncomplexed DB18C6 are studied in implicit methanol, implicit water, and in the gas phase. With conformations optimized in each condition, the conformations of DB18C6 in complex with ammonium ion are studied computationally to explore its features in the polar solvent methanol that is chosen to mimic an amphipathic protein. Binding is also examined experimentally using NMR to determine affinity. Although water is a preferred solvent for studies that aim to shed light on protein behaviors, the limited solubility of DB18C6 in water (< 0.1 mM [1, 18]) precludes its use in many experimental approaches to binding studies. Density functional theory (DFT) is used to calculate the binding energy of ammonium ion with DB18C6 in the gas phase and in the implicit solvents. As found by Choi et al. [19], who examined the ion selectivity of DB18C6 with cations Li^+, Na^+, K^+, Rb^+, and Cs^+ using a conductor-like polarizable continuum model (CPCM) [20], an implicit solvation model was found to be suitable for calculating the solvation energy of DB18C6.

Methods

Experimental methods

All experiments used deuterated methanol, CD_3OD 99.8%, and $^{15}NH_4Cl$, 98% + obtained from Cambridge Isotope Laboratories. Dibenzo-18-crown-6 98% was from Sigma-Aldrich. DB18C6 methanol solution was made at its solubility limit of 0.001 M [1, 18] by dissolving 0.18 mg DB18C6 in 0.5 mL MeOD with very gentle heating. ^{1}H-NMR spectra were collected at 500 MHz field strength on a Bruker Avance III instrument equipped with a QCI cryoprobe, at controlled

temperature of 22 °C. A 10 mM stock of $^{15}NH_4Cl$ was made by dissolving 0.27 mg of anhydrous $^{15}NH_4Cl$ in 0.5 mL of deuterated methanol. ^{1}H-NMR reference spectra of the separate DB18C6 and $^{15}NH_4Cl$ stock solutions were obtained before each titration experiment. Titration experiments used 5-uL increments of $^{15}NH_4Cl$ solution added to 1 mM crown ether solution. After each addition, the ^{1}H-NMR spectrum was collected.

The treatment of ligand-binding data used here follows that of Klotz [21]. The definition of the association binding constant, K_a, is the concentration of complex $[AB]$ divided by the product of the concentrations of free ligand, $[A_f]$, and free target, $[B_f]$:

$$K_a = \frac{[AB]}{[A_f][B_f]} \tag{1}$$

This expression asserts, through its use of [AB] to describe the complex, that the binding process observes a 1:1 interaction between host and guest; this assumption is here shown by experiment to be accurate for the present case. As the amounts of free target and free ligand are unknown to the observer, the following relation uses the conservation of mass to express the concentration of free reactants as the difference between the total concentration of ligand and the concentration of bound ligand, under the 1:1 assumption.

$$[A_f] = [A_t] - [AB] \tag{2}$$

$$[B_f] = [B_t] - [AB] \tag{3}$$

To solve for $[AB]$, Eqs. (2) and (3) are substituted into Eq. (1), and the resulting equation is rearranged using the quadratic formula. Equation (4) defines fractional site occupancy, $\overline{v}$, the fraction of binding sites on target B that are occupied by ligand A. As defined here, $\overline{v}$ is the experimental observable assuming 1:1 binding of ligand A on target B, which is confirmed under "Experimental results".

$$\overline{v} = \frac{[AB]}{[B_t]} \tag{4}$$

Given Eqs. (1)–(4) above, the following relation relates K_a to the experimental observable, $\overline{v}$,

$$\overline{v} = \frac{K_a([A_t] - [AB])}{1 + K_a([A_t] - [AB])} \tag{5}$$

where $[A_t] = [^{15}NH_4Cl]$, K_a is the association binding constant, and $[AB] = [DB18C6\bullet^{15}NH_4Cl]$ as observed experimentally. Equation (4) is used to find K_a by fitting it to the experimental data.

Computational methods

DB18C6, NH_4^+, and their complex were studied by DFT with the functionals B3LYP, B3LYP-D, B3LYP-D3, and M05-2X [22–29]. For a non-covalent interaction, a dispersion correction must be included in the choice of functional. Computations were performed using cc-pVTZ and aug-cc-pVTZ basis sets [30, 31]. Gas phase computations were performed using Psi4 v1.0.54 [32, 33] and Gaussian 09 [34] software packages. All calculations with solvent were done using Gaussian 09 and Gaussian 16 [35] with the M05-2X functional and cc-pVTZ basis set. A table of the computational details is included in the Supporting Information. Six conformers of DB18C6 were determined and optimized in this study. These six conformers (Fig. 2) match qualitatively (i.e., structurally) to previously determined structures in the literature [12–16]: structures I and II correspond with reference 12, III with reference 13, IV with reference 14, V with reference 15, and VI with reference 16. For the complexed structures, NH_4^+ was placed at the center of mass of DB18C6 and then fully optimized. Frequency calculations were performed to confirm minima and compute thermodynamic values.

The theoretical methods used in the calculations of binding energy are detailed in Supporting Information. As described there, binding energies have been corrected to include geometry relaxation in addition to solvent interaction effects and counterpoise methods to account for basis set superposition errors. Methanol and water solvation effects are accounted for implicitly using the universal solvation model (SMD) [36]. This model is based on the solute electron density and polarizable continuum model in which solvent is treated implicitly as a continuous medium surrounding the solute, with dielectric constants used to model the electrostatic effects of solvent.

Results

Experimental results

$^{15}NH_4Cl$ was chosen as ligand, anticipating that both forward ($^{15}NH_4Cl$ into DB18C6) and reverse (DB18C6 into $^{15}NH_4Cl$) titrations might be required to resolve unambiguously both the affinity and molar ratio of binding by using both ^{1}H and ^{15}N NMR spectra, respectively (Klotz [21]). However, the forward titration results reported here clearly resolve both binding parameters, as described below; thus, reverse titrations were not carried out. Peak assignments for protons in the ^{1}H-NMR spectrum of DB18C6 in MeOD at 500 MHz (Figs. 1 and 2A) were determined by spectral prediction using MNova [37], and are in agreement with

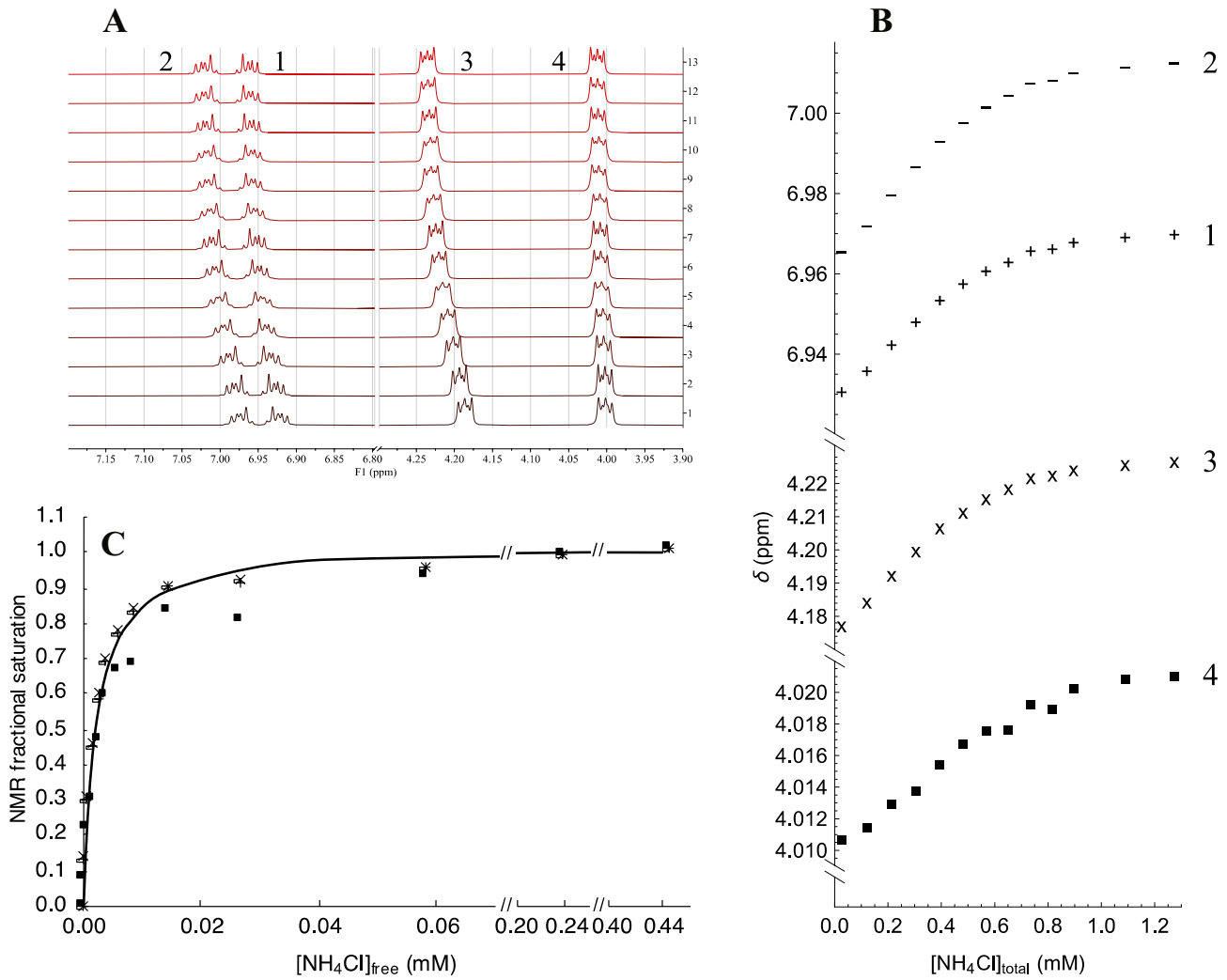

Fig. 2 Titration of DB18C6 with $^{15}NH_4Cl$ monitored by ^{1}H-NMR. **A** Raw data. ^{1}H-NMR spectra acquired upon titration of 1.0 mM DB18C6 in methanol with sequential 5 uL aliquots from a 10 mM $^{15}NH_4Cl$ stock in methanol. Spectra numbered 1–13 at the right correspond to final total. $^{15}NH_4Cl$ concentrations of 0, 0.099, 0.196, 0.291, 0.385, 0.476, 0.566, 0.654, 0.741, 0.826, 0.909, 1.111, and 1.304 mM, respectively. F1, NMR frequency channel one. **B** Quantification. Chemical shift (δ, ppm) is plotted against total ligand concentration for protons 1, 2, 3, and 4 (cross, dash, x, square, respectively). Note the discontinuous y-axis values required to accommodate all four protons on one plot. **C** Binding isotherm. As described in the text, the apparent fractional progress of chemical shift for protons 1, 2, 3, and 4, is plotted vs. free ammonium chloride concentration using the symbols of panel **B**. Note the discontinuous x-axis values as apparent saturation is approached. The solid line is calculated using Eq. (5) with $K_a = 5 \times 10^5 M^{-1}$, corresponding to $K_d = 2 \times 10^{-6} M^{-1}$

those reported previously by Kriz [15] in nitrobenzene-d5 at 300 MHz field strength. The NMR spectra are consistent with a single averaged conformation of DB18C6 in methanol, as expected for a relatively small molecule (MW ~ 300 Da) whose conformational transitions are likely to be fast on the NMR timescale.

Chemical shift changes during the titration were used to monitor the binding process (Fig. 2B). Addition of $^{15}NH_4Cl$ causes a uniform, progressive change in the chemical shifts of all four unique DB18C6 ^{1}H resonances, without any splitting of resonances. This result indicates that rapid exchange on the NMR timescale among potential conformers is maintained in the complex, similar to the rapid conformational exchange observed in the free crown. Sequential additions of $^{15}NH_4Cl$ result in progressive chemical shift changes for all four unique proton resonances of DB18C6, reflecting binding of the $^{15}NH_4^+$ ion to the crown. Although all four protons track the titration, the magnitude of change in chemical shift differs among them, being especially large for methylene proton 3 and very small for methylene proton 4. Quantitatively, all four protons respond similarly and reach limiting values of their chemical shifts upon addition of 1.1 to 1.3 mM $^{15}NH_4Cl$ to 1 mM DB18C6. This result reveals that full occupancy of binding sites on DB18C6 requires

addition of only one molar equivalent of $^{15}NH_4Cl$ per crown, indicating that the molar ratio of partners in the complex is 1:1, as expected from all prior work on this crown [2–4].

The fact that saturation is achieved when approximately one molar equivalent of total ammonium chloride is added indicates additionally (Klotz [21]) that the affinity of the interaction is significantly stronger than the experimental concentrations (i.e., K_d is significantly lower than 1 mM). Under such conditions, the binding process proceeds in the so-called stoichiometric limit of the titration, i.e., the ligand adds to the target in a mole-for-mole manner because the concentrations of both reagents are far above K_d [21].

This behavior reflects operation of Le Chatelier's principle as applied to mass, also called mass action. Based on the stoichiometric binding result, the 1:1 binding model was used to calculate the concentration of free ligand at each step of the titration, with the averaged ppm values at the two highest ligand concentrations taken as an estimate for the ppm values at full saturation in order to normalize all values and thus determine the fractional progress of the binding process. The resulting data, i.e., fractional saturation as a function of free ligand concentration, are reasonably well fit by a K_d value of ~ 2×10^{-6} M (Fig. 2C). However, because the titration occurs in the stoichiometric limit, the subtraction of total ligand minus bound ligand required to determine free ligand concentration is error prone and results in concentrations that are relatively small, limiting the goodness of fit. The fit is also affected by normalization using the two highest ppm values, which clearly are approaching saturation but may not truly represent 100% saturation. Higher concentrations of ligand or target cannot be achieved due to solubility limits.

The original reason for using $^{15}NH_4Cl$ was the anticipated need to carry out reverse titrations (i.e., with a fixed concentration of $^{15}NH_4Cl$ titrated incrementally with DB18C6) in order to establish the molar ratio of reactants. However the finding that titration of DB18C6 with $^{15}NH_4Cl$ proceeds in the stoichiometric limit and with a clear breakpoint near molar ratio of 1:1 obviates the reverse titration. This result further indicates that the concentrated stock solution of DB18C6 that would be required as titrant in a reverse titration would be beyond its solubility limit.

Computational results

Geometry optimizations and single-point energy computations were performed with the uncomplexed crown in the gas phase, in implicit methanol, and in implicit water. Multiple conformers of DB18C6 have been reported previously using experimental and/or computational methods [12–16]. The coordinates of the published structures were used as a starting point here for computations optimized at the level of theory described in the computational methods section.

The computations led to six optimized (i.e., locally minimal) conformers of DB18C6 in each of the three solvent conditions, as shown in Fig. 3A for the gas phase; the symmetry point group of each structure is also indicated. Cartesian coordinates, dipole moments, absolute energies, and RMSD values for all structures are reported in the Supporting Information. Visually, the optimized conformers do not differ significantly among the gas and the two solvents. RMSD values were calculated to quantify the difference between conformers in gas phase and in solvents. The RMSD values are small (0.0355–1.9582 Å), indicating that the structures do not differ substantially when including implicit solvent, although the conformer with the lowest energy differs in the three conditions. The relative energies of all conformers in all conditions are reported in Table 1, where the lowest-energy conformer in each condition is assigned zero relative energy, and relative energies are applicable only within columns. The results indicate structure I as the lowest-energy conformer in the gas phase and structure III as the lowest-energy conformer in implicit water or implicit methanol. Structure III is approximately W shaped when viewed from the side, and structure I resembles a W in which the middle and both ends are slightly flattened (Fig. 3A). When viewed from above both structures I and III have central cavities that are larger than in structures II, IV, and VI; only structure V has a similarly large cavity, as judged by the distance between the carbon-4 protons that flank the central cavity (Table 2). In the gas phase, structure III has the largest dipole moment of 1.92 Debye, indicating it is expected to interact favorably with polar solvents.

For each of the six low-energy conformers in the three conditions, an NH_4^+ ion was placed at the center of mass of DB18C6 and optimized in the cavity. DFT calculations were carried out to determine the lowest-energy conformer when complexed with NH_4^+. The calculations also optimize the position of the ammonium ion with respect to the crown. The resulting relative energies of complexes are reported in Table 1; the lowest-energy structures in implicit methanol that are relevant for the present experimental analysis are shown in Fig. 3B. In contrast to uncomplexed DB18C6, when NH_4^+ is bound the lowest-energy conformer in all three conditions, by over 2 kcal mol^{-1}, is conformer III, with only structure V approaching similar energy values, as is also the case for uncomplexed DB18C6. This finding presumably reflects the size of the central cavity in structures III (11.07 Å benzene-to-benzene distance) and V (10.99 Å), which may best accommodate the ion. Structure VI, with the same cavity size as structure III, has a slightly larger energy than structure V, presumably because the chair-like conformation of VI displaces some of the interacting atoms on one side of the host, as evident from the side view in Fig. 3B. The optimized structures of the complex show that the ion is located in the central cavity of the crown when viewed

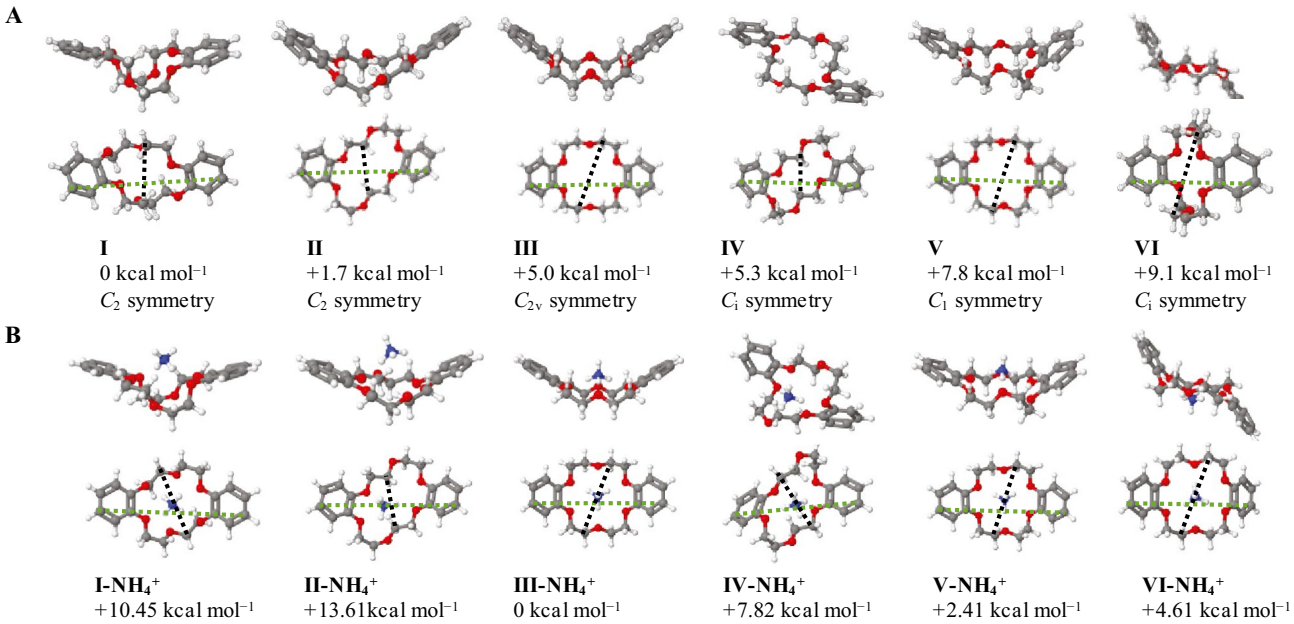

Fig. 3 Gas phase structures and relative stabilities of DB18C6 and its NH_4^+ complex. A side view (upper structures in each row) and a top view (lower structures) are shown for six conformers (I to VI). The black dashed lines measure the shortest distance between carbons that flank the central cavity of the crown. The green dashed lines measure the benzene ring distance from proton 1 of one benzene ring to proton 1 of the benzene ring on the opposite side of the cavity. The structure with the lowest stability is assigned an energy value of 0 kcal mol^{-1}. **A** Uncomplexed DB18C6 in gas phase. The symmetry point group is listed below each conformer. **B** DB18C6-NH_4^+ complex in implicit methanol

from above, as expected, although two-dimensional views do not accurately describe its position because the crown is not planar. Side views show that the ion is displaced upward from the central cavity, occupying a position approximating the center of mass of the complex as judged by the Cartesian coordinates of the ammonium nitrogen atom (data not shown). The NH_4^+ ligand in structure III is closest to the center of mass in the gas phase, implicit water, and implicit methanol. Dipole moment calculations for the complexes (Supplemental Table S2) show a trend in which the ammonium ion reduces the larger dipole moments of the uncomplexed crowns. In the gas phase, structures III and V have the largest dipole moments at 1.92 and 1.65 Debye respectively. In contrast, the complexed structures III and V have the smallest dipole moments at 0.56 and 0.41 respectively, indicating that the addition of ammonium ion balances the charge distribution. Consistent with this pattern, complexed structures III and V are the lowest-energy conformers in both implicit solvents.

Table 1 Relative conformer energies. Energies of DB18C6 and DB18C6-NH_4^+ complexes are given in kcal mol^{-1}, with the lowest-energy structure in each condition given a value of 0.00 kcal mol^{-1}

Conformer	Gas	Water	Methanol
I	0.00	+3.51	+2.48
II	+1.71	+5.06	+4.58
III	+4.99	0.00	0.00
IV	+5.27	+7.60	+7.82
V	+7.79	+1.94	+2.41
VI	+9.08	+4.43	+4.61
I-NH_4^+	+5.24	+7.57	+10.45
II-NH_4^+	+14.12	+12.22	+12.58
III-NH_4^+	0.00	0.00	0.00
IV-NH_4^+	+15.17	+13.82	+15.10
V-NH_4^+	+3.27	+1.86	+2.38
VI-NH_4^+	+6.36	+4.51	+5.18

To quantify the structural changes upon guest binding, the benzene ring distances and the shortest distance across the crown cavity were measured in the gas phase, implicit water, and implicit methanol in presence and absence of ammonium ion (Table 2). The geometries alter when accommodating the ammonium ion, indicating that the crown is flexible, as expected, and that more than one crown conformer can accommodate the ion. In the gas phase, the binding of ammonium ion causes an increase in the benzene ring distances of ~ 0.2 to ~ 0.7 Å for all structures. In implicit water, the increases are much smaller (~ 0 to ~ 0.3 Å), and two instances of contraction occur upon binding. In implicit methanol, only structure III displays a substantial increase; all other distance changes are very small, whether negative or positive. The increase for structure III correlates with a

Table 2 Distances within DB18C6 and DB18C6-NH_4^+. Benzene ring distances are measured from proton 1 (as numbered in Fig. 1) of one benzene ring to proton 1 of the benzene ring across the cavity. Cavity distances are measured between the closest carbon atoms flanking the cavity

	Benzene ring distance (Å)			Shortest crown cavity distance (Å)		
Conformer	Gas	Water	Methanol	Gas	Water	Methanol
I	11.62	11.74	11.72	4.34	4.46	4.50
I-NH_4^+	11.83	12.02	11.35	6.32	5.71	5.65
II	10.63	11.09	11.16	4.30	4.26	4.25
II-NH_4^+	11.37	11.02	11.21	5.56	4.48	4.44
III	10.65	10.84	10.80	6.64	6.71	6.68
III-NH_4^+	11.14	11.11	11.07	6.65	6.69	6.66
IV	10.76	10.62	10.69	4.43	4.63	4.60
IV-NH_4^+	11.02	10.26	10.27	4.71	4.77	4.78
V	10.72	10.94	10.90	6.58	6.73	6.70
V-NH_4^+	11.09	10.94	11.08	6.77	6.76	6.74
VI	10.86	10.93	10.96	6.74	6.89	6.89
VI-NH_4^+	11.11	10.97	11.07	6.98	6.87	6.92

slightly flatter and more open structure that is expected to relieve the steric clash that would otherwise occur between the ion and the carbon-4 protons. Although the angle between benzene rings in structure III increases from 108.9 degrees to 109.7 degrees upon complex formation in implicit methanol, the carbon-4 protons move rather little. The shortest distance across the crown cavity is essentially unchanged for conformer III in all three conditions, whereas all other conformers display a larger change in this distance in one or more condition.

Binding energies for NH_4^+ interaction with DB18C6 were calculated for the six optimized structures in the three solution conditions using the counterpoise correction method including geometry correction as detailed in Supporting Information. The binding energies are reported in Table 3, where negative values represent favorable interactions. These binding energies are not to be confused with free energy changes or enthalpy changes upon ligand binding; rather the term "binding energies" is chosen to conform with literature cited here for comparison. The ammonium ion has favorable calculated binding energies with all six optimized conformers in the gas phase and in both water and methanol implicit solvents. Structure III has the most favorable binding energy in the gas phase, consistent with its being the most stable conformer, whereas structure V has the most favorable binding energy in both water and methanol implicit solvents. Structure V has a conformer energy very similar to that of structure III in both solvents. The binding energy for ammonium ion with DB18C6 ranges from − 50.23 to − 67.10 kcal mol^{-1} in the gas phase, consistent with reported energies for alkali metals binding to the crown in the gas phase [38, 39], which range from ~ 50–100 kcal mol^{-1}. In the implicit solvents, structures III, V, and VI have similar, and favorable, binding energies, ranging from − 11.13 to − 11.30 kcal mol^{-1} in water and from − 12.02 to − 12.66 kcal mol^{-1} in methanol.

The binding free energies calculated with counterpoise correction, ΔG_{bind}^{CP}, indicate that all conformers show strong favorable interaction with ammonium ion in the gas phase, with structure III having $\Delta G_{bind}^{CP} = -52.8$ kcal mol^{-1}. In

Table 3 Binding energies of DB18C6-NH_4^+ complexes

	Gas	Water	Methanol	Gas	Water	Methanol
Conformer	ΔE_{BSSE} [a]	ΔE_{BSSE}	ΔE_{BSSE}	ΔE_{bind}^{CP} [b]	$\Delta E_{bind,solv}^{CP}$ [c]	$\Delta E_{bind,solv}^{CP}$ [d]
I	1.60	1.56	1.14	− 57.04	− 7.34	− 5.59
II	1.23	0.77	0.93	− 50.23	− 5.04	− 5.36
III	1.77	1.78	1.78	− 67.10	− 11.19	− 12.56
IV	1.17	0.65	0.66	− 52.79	− 6.59	− 6.13
V	1.74	1.73	1.73	− 66.65	− 11.30	− 12.66
VI	1.73	1.74	1.72	− 64.87	− 11.15	− 12.02

[a]BSSE energy, difference between the counterpoise-corrected binding energy and the binding energy with no corrections

[b]Counterpoise-corrected binding energy of the complex in vacuum

[c]Counterpoise-corrected binding energy of the complex in implicit water solvent

[d]Counterpoise-corrected binding energy of the complex in implicit methanol solvent

implicit solvent, only two structures are slightly favorably bound, with $\Delta G_{bind}^{CP} = -0.2$ kcal mol^{-1} for structure VI in water and -0.3 kcal mol^{-1} for structure III in methanol. All ΔG_{bind}^{CP} values for the crown—ammonium ion complexes—are reported in the Supporting Information. The values are all close to zero and should be regarded as largely qualitative because the potential energy surfaces are shallow, implying poorly defined minima.

This difference in binding energies between the gas phase, where the favorable energy is greater than 50 kcal mol^{-1} in magnitude, and the two implicit solvents methanol and water, where it ranges from -5.04 to -12.66 kcal mol^{-1}, can be accounted for largely by the computed electronic solvation energies of ammonium ion in water or methanol, NH_4^+, $\Delta E_{solv} = E_s - E_g$. Before BSSE correction, ΔE_{solv} is -82.2 kcal mol^{-1}, in line with previous work [40]; in comparison, neutral ammonia in water is reported to have ΔE_{solv} -3.4 kcal mol^{-1}. This large difference in ΔE_{solv} reflects the much larger response expected for a system of polarizable implicit solvent and a charged ion. The equivalent calculations for free DB18C6 and for its complex with ammonium ion yield computed electronic solvation energies ΔE_{solv} of -22.9 and -49.2 kcal mol^{-1}, respectively. ΔE_{solv} for uncharged DB18C6 alone is unsurprisingly smaller because it is neutral, whereas the complex is charged due to the presence of NH_4^+. However, the ammonium ion is contained inside the crown, shielding its interactions with solvents in the implicit continuum compared to free ammonium ion. The difference between the binding energies in the gas phase vs. in implicit solvent is thus due to one main effect, the large ΔE_{solv} of NH_4^+.

Conclusions

Experimental titration of DB18C6 with $^{15}NH_4Cl$ monitored by ^{1}H-NMR indicates that the ammonium cation binds strongly to DB18C6 in methanol, with a binding (dissociation equilibrium) constant, K_d, that is at least as strong as 10^{-6} M. This result is consistent with values reported in the literature for other ammonium salts binding to DB18C6 and/or for ammonium ion binding in other solvents [4, 7, 8]. Assuming that the rate constant for association of the ion with the crown is under diffusion control, which is a reasonable assumption for small molecules including a host that bears no full formal charges [41], the dissociation equilibrium constant is equal to the ratio of rate constants (k_{off}/k_{on}) and can be used to predict the dissociation rate constant. Using 10^8 M^{-1} s^{-1} as a reasonable estimate of the diffusion-limited value of k_{on} for molecules of this size, the resulting value of k_{off} is at least 10^2 s^{-1}. For this unimolecular dissociation process, this off-rate constant implies a complex half-life of less than 7 ms [41]. This result is consistent with the NMR data, which indicate that the bound and free states are in fast exchange on the NMR time scale.

The results of DFT calculations predict that the binding energy for ammonium ion and DB18C6 is strong also in the gas phase. In contrast, the calculated ammonium ion binding energy with DB18C6 in implicit solvent, whether water or methanol, is only slightly favorable. These results reflect in part the limits of accuracy when solvents are treated implicitly. Choi et al. [19] studied cations Li^+, Na^+, K^+, Rb^+, and Cs^+ with DB18C6 in implicit water and observed an increase in the alkali metal-to-oxygen distance that they attributed to a weakening of the cation-oxygen attraction in the solvent dielectric field. They suggest that continuum (implicit) solvent models do not account well enough for the substantial hydration energies of first shell water molecules, which arrange their oxygen atoms toward the cation. Such effects may also be at work in the present study, where the calculated binding energy for ammonium ion with DB18C6 is slightly more favorable in methanol than in water, presumably reflecting that water is a better solvent than methanol for free ammonium ion due to its higher polarity, as suggested by the results of Choi et al. for the alkali metal ions. The results of the present work provide the essential foundation for studies of this system and related crowns, which have been initiated using molecular dynamics simulations.

It is important to note that the calculated binding energies in Table 3 cannot be related directly to, nor do they predict, binding free energies or internal energies. The calculated energies neglect some realistic solvent properties, and they may fail to capture some sources of enthalpic and entropic contributions to the interaction that arise from both the free and bound interactants, as well as from the solvent itself in both free and bound states. All these contributions can be considered *cryptic* in the sense that they are not generally observable by experiment. Water is expected to be a more effective competitor than methanol for binding to ammonium ion. The competition between solvation and binding, in turn, is expected to have the effect of reducing the net free energy of binding in water compared to methanol.

Probably the single most important lesson of the host–guest chemistry, one for which Lehn, Cram, and Pedersen won the Nobel Prize in 1987, is that *the bonds between host and guest are identical whether a host is pre-organized or not, yet both the affinity and specificity for a guest can be orders of magnitude different* [42]. This fact leads to the following profound conclusion that applies generally to all molecular interactions: bonding between the partners does not predict their affinity and in fact need scarcely be related to affinity; this can be shorthanded as *bonding does not predict binding*. Thermodynamic data tabulated years ago by Klotz [21] showed that some very favorable interactions (e.g., $\Delta G \cong -16$ kcal/mol

for Cro repressor/operator DNA binding and ≅ − 12 kcal/mol Cro/non-operator DNA) have positive enthalpy changes (≅ + 1 kcal/mol for Cro/operator DNA; ≅ + 4 kcal/mol for Cro/non-operator DNA). A similar pattern has since been found for many other biomolecular interactions. An implication of this fact is that structural analysis of bonding between partners cannot inform us about their affinity. The basic reason is that structural analysis of intermolecular bonds neglects all the rest of the system and its many contributions, both favorable and unfavorable, to both enthalpy and entropy, in both bound and free states.

Supplementary Information The online version contains supplementary material available at https://doi.org/10.1007/s11224-022-02017-8.

Author contribution Study conception and design: J. C. and D. B. M.; materials preparation and NMR data collection: B. S. and I. P.; computational data coysellection: B. S., B. M., D. B. M., D. R. All authors contributed to data analysis. The first draft of the manuscript was written by B. S. and J. C., and all authors contributed to intermediate versions. All authors have read and approved the final manuscript.

Funding B. M. and D. R acknowledge access to modeling facilities supported by the Czech research infrastructure for systems biology C4SYS (project no. LM2015055) and computational resources provided by the CESNET LM2015042 and the CERIT Scientific Cloud LM2015085, provided under the program "Projects of Large Research, Development, and Innovations Infrastructures." This work was carried out when B. S. was an undergraduate research participant in an NSF REU Training Site in Molecular Biophysics supported by awards DBI13-58737 and DBI16-59726 to J.C.

Data availability The data generated and/or analyzed during this study are available from the corresponding authors on request.

Declarations

Conflict of interest The authors declare no competing interests.

References

1. Pedersen CJ (1967) Cyclic polyethers and their complexes with metal salts. J Am Chem Soc 89:7017–7036. https://doi.org/10.1021/ja01002a035
2. Pedersen CJ (1967) Cyclic polyethers and their complexes with metal salts. J Am Chem Soc 89:2495. https://doi.org/10.1021/ja00986a052
3. Pedersen CJ, Frensdorff HK (1972) Macrocyclic polyethers and their complexes. Angew Chemie Int Ed English 11:16–25. https://doi.org/10.1002/anie.197200161
4. Izatt RM, Pawlak K, Bradshaw JS, Bruening RL (1991) Thermodynamic and kinetic data for macrocycle interaction with cations and anions. Chem Rev 91:1721–2085. https://doi.org/10.1021/cr00008a003
5. De Jong F, Reinhoudt DN (1980) Stability and reactivity of crown-ether complexes. Adv Phys Org Chem 17:279–433. https://doi.org/10.1016/S0065-3160(08)60130-6
6. Shchori E, Nae N, Jagur-Grodzinski J (1975) Stability constants of complexes of a series of metal cations with 6,7,9,10,17,18,20,21-octahydrodibenzo[b,k][1,4,7,10,13,16]hexa-oxa-cyclo-octadecin (dibenzo-18-crown-6) in aqueous solutions. J Chem Soc Dalt Trans 2381. https://doi.org/10.1039/dt9750002381
7. Angelis K, Brezina M, Koryta J (1973) Electrode processes of ammonium ion and its complexes with macrocyclic ligands in propylene carbonate and acetonitrile. J Electroanal Chem 45:504–507. https://doi.org/10.1016/S0022-0728(73)80064-6
8. Izutsu K, Nakamura T, Murayama T, Fujinaga T (1978) The complexing of the ammonium Ion in acetonitrile with other solvents. Investigation Using a Cation-sensitive Glass Electrode. Bull Chem Soc Jpn 51:2905–2908. https://doi.org/10.1246/bcsj.51.2905
9. Frensdorff HK (1971) Stability constants of cyclic polyether complexes with univalent cations. J Am Chem Soc 93:600–606. https://doi.org/10.1021/ja00732a007
10. Fielding L (2007) NMR methods for the determination of protein-ligand dissociation constants. Prog Nucl Magn Reson Spectrosc 51:219–242. https://doi.org/10.1016/j.pnmrs.2007.04.001
11. Live D, Chan SI (1976) Nuclear magnetic resonance study of the solution structures of some crown ethers and their cation complexes. J Am Chem Soc 98:3769–3778. https://doi.org/10.1021/ja00429a006
12. Hoijemberg PA, Moss RA, Feinblum DV, Krogh-Jespersen K (2014) O-ylide and π-complex formation in reactions of a carbene with dibenzo and monobenzo crown ethers. J Phys Chem A 118:6230–6238. https://doi.org/10.1021/jp506154s
13. Perekalin DS, Babak MV, Novikov VV et al (2008) A new approach to the photochemically controlled crown ethers: (tetramethylcyclobutadiene)cobalt complexes with benzo-15-crown-5 and dibenzo-18-crown-6. Organometallics 27:3654–3658. https://doi.org/10.1021/om7002688
14. Bright D, Truter MR (1970) Crystal structures of complexes between alkali-metal salts and cyclic polyethers. Part I. Complex formed between rubidium sodium iso-thiocyanate and 2,3,11, I 2-dibenzo-l,4,7,4 0,13,16-hexaoxocyclo-octadeca- 2, ll-diene ('dibenzo-18-crown-6'). J Chem Soc 13:1544–1550. https://doi.org/10.1039/J29700001544
15. Kriz J, Dybal J, Makrlik E, Budka J (2008) Interaction of hydronium ion with dibenzo-18-crown-6: NMR, IR, and theoretical study. J Phys Chem A 112:10236–10243. https://doi.org/10.1021/jp805757d
16. Dapporto P, Paoli P, Matijasic I, Tusek-Bozic L (1996) Crystal structures of complexes of ammonium and potassium hexafluorophosphate with dibenzo-18-crown-6. Molecular mechanics studies on the uncomplexed macrocycle. Inorganica Chim Acta 252:383–389. https://doi.org/10.1016/s0020-1693(96)05407-2
17. Bright D, Truter MR (1970) Crystal structure of a cyclic polyether complex of alkali metal thiocyanate. Nature 225:176–177. https://doi.org/10.1038/225176a0
18. Kolthoff IM (1979) Application of macrocyclic compounds in chemical analysis. Anal Chem 51:1–22. https://doi.org/10.1021/ac50041a001
19. Min Choi C, Heo J, Joon Kim N (2012) Binding selectivity of dibenzo-18-crown-6 for alkali metal cations in aqueous solution: a density functional theory study using a continuum solvation model. Chem Cent J 6:1–8. https://doi.org/10.1186/1752-153X-6-84
20. Barone V, Cossi M (1998) Quantum calculation of molecular energies and energy gradients in solution by a conductor solvent model. J Phys Chem A 102:1995–2001. https://doi.org/10.1021/jp9716997
21. Klotz IM (1997) Ligand-receptor energetics : a guide for the perplexed. Wiley, New York
22. Becke AD (1993) Density-functional thermochemistry. III. The role of exact exchange. J Chem Phys 98:5648–5652. https://doi.org/10.1063/1.464913
23. Lee C, Yang W, Parr RG (1988) Development of the Colle-Salvetti correlation-energy formula into a functional of the electron density. Phys Rev B 37:785–789. https://doi.org/10.1103/PhysRevB.37.785

24. Vosko SH, Wilk L, Nusair M (1980) Accurate spin-dependent electron liquid correlation energies for local spin density calculations: a critical analysis. Can J Phys 58:1200–1211. https://doi.org/10.1139/p80-159
25. Stephens PJ, Devlin FJ, Chabalowski CF, Frisch MJ (1994) Ab initio calculation of vibrational absorption and circular dichroism spectra using density functional force fields. J Phys Chem 98:11623–11627. https://doi.org/10.1021/j100096a001
26. Grimme S (2004) Accurate description of van der Waals complexes by density functional theory including empirical corrections. J Comput Chem 25:1463–1473. https://doi.org/10.1002/jcc.20078
27. Grimme S (2006) Semiempirical GGA-type density functional constructed with a long-range dispersion correction. J Comput Chem 27:1787–1799. https://doi.org/10.1002/jcc.20495
28. Grimme S, Antony J, Ehrlich S, Krieg H (2010) A consistent and accurate ab initio parametrization of density functional dispersion correction (DFT-D) for the 94 elements H-Pu. J Chem Phys 132:154104. https://doi.org/10.1063/1.3382344
29. Zhao Y, Schultz NE, Truhlar DG (2006) Design of density functionals by combining the method of constraint satisfaction with parametrization for thermochemistry, thermochemical kinetics, and noncovalent interactions. J Chem Theory Comput 2:364–382. https://doi.org/10.1021/ct0502763
30. Dunning TH (1989) Gaussian basis sets for use in correlated molecular calculations. I. The atoms boron through neon and hydrogen. J Chem Phys 90:1007–1023. https://doi.org/10.1063/1.456153
31. Kendall RA, Dunning TH, Harrison RJ (1992) Electron affinities of the first-row atoms revisited. Systematic basis sets and wave functions. J Chem Phys 96:6796–6806. https://doi.org/10.1063/1.462569
32. Turney JM, Simmonett AC, Parrish RM et al (2012) Psi4: an open-source ab initio electronic structure program. WIREs Comp Mol Sci 2:556–565. https://doi.org/10.1002/wcms.93
33. Parrish RM, Burns LA, Smith DG et al (2017) PSI4 1.1: an open-source electronic structure program emphasizing automation, advanced libraries, and interoperability. J Chem Theory Comput 13:3185–3197. https://doi.org/10.1021/acs.jctc.7b00174
34. Frisch MJ, Trucks GW, Schlegel HB et al (2009) Gaussian 09 Revision A.02, Gaussian Inc., Wallingford, CT
35. Frisch MJ, Trucks GW, Schlegel HB et al (2016) Gaussian 16 Revision C.01, Gaussian Inc., Wallingford, CT
36. Marenich AV, Cramer CJ, Truhlar DG (2009) Universal solvation model based on solute electron density and on a continuum model of the solvent defined by the bulk dielectric constant and atomic surface tensions. J Phys Chem B 113:6378–6396. https://doi.org/10.1021/jp810292n
37. Willcott MR (2009) MestRe Nova. J Am Chem Soc 131:13180. https://doi.org/10.1021/ja906709t
38. Thompson MA, Glendening ED, Feller D (1994) The nature of K+/crown ether interactions: a hybrid quantum mechanical-molecular mechanical study. J Phys Chem 98:10465–10476. https://doi.org/10.1021/j100092a015
39. Glendening ED, Feller D, Thompson MA (1994) An ab initio investigation of the structure and alkali metal cation selectivity of 18-crown-6. J Am Chem Soc 116:10657–10669. https://doi.org/10.1021/ja960469n
40. Saielli G (2010) Differential solvation free energies of oxonium and ammonium ions: insights from quantum chemical calculations. J Phys Chem A 114:7261–7265. https://doi.org/10.1021/jp103783j
41. Cantor C, Schimmel PR (1980) Biophysical chemistry, 3rd ed. W. H. Freeman, San Francisco
42. Carey J (2022) Affinity, specificity, and cooperativity of DNA binding by bacterial gene regulatory proteins. Int J Mol Sci 23. https://doi.org/10.3390/ijms23010562